Antenna Tilt Adaptation for Multi-Cell Massive MIMO Systems

Anzhong Hu

Abstract—**This letter proposes an antenna tilt adaptation approach for multi-cell massive multiple-input multiple-output systems. The asymptotic spectral efficiency of the system with pilot contamination in the limit of the antennas is first derived. The analysis demonstrates that the spectral efficiency is a concave function of the tilts with some specific requirements being satisfied. As a result, a gradient descent-based method is proposed to approach the optimal tilt. Numerical results verify that the proposed approach performs better than a traditional low-complexity approach.**

Index Terms—**Active antennas, adaptive antennas, MIMO systems, optimization methods, antenna gain.**

I. Introduction

MASSIVE multiple-input multiple-output (MIMO) systems can provide high spectral efficiency and energy efficiency, and may be implemented in the future wireless systems [1], [2]. However, the limited channel coherence interval makes the orthogonal pilots too long to be employed, which causes interference in channel estimation. Furthermore, this interference constrains the performance improvement of massive MIMO systems, and this phenomenon is named pilot contamination. In order to mitigate the interference in massive MIMO systems, several methods have been proposed [3]. However, these methods only consider the transmission in the horizontal plane, while the degree of freedom (DoF) in the vertical dimension has not been used.

Recently, antenna tilt was designed to improve the spectral efficiency of MIMO systems [4]–[12]. Antenna tilt is the elevation angle of the antenna pattern, and can be adjusted electronically to control the antenna gain. Hence, with the adaptation of the tilt, MIMO systems can take use of the DoF in the three-dimensional space, and is able to mitigate the interference more efficiently. With the knowledge of the locations of the UTs, the antenna tilt of the base station (BS) is dynamically adjusted to maximize the sum rate in [9], [10]. When only the statistics of the locations of the UTs are available and the tilt is fixed, the tilt is designed to maximize the sum rate in [11]. However, these approaches rely on perfect channel state information (CSI), which is not available when pilot contamination is severe. Moreover, the approaches in [9] and [10] necessitate exhaustive search. In [12], the antenna tilt is adjusted to maximize the sum rate for single cell MIMO system, which means the interference is not handled. Hence, these tilt design approaches are not suitable for multi-cell massive MIMO systems.

Manuscript received July 14, 2017; accepted August 8, 2017. Date of publication August 18, 2017; date of current version November 9, 2017. This research was supported by Zhejiang Provincial Natural Science Foundation of China under Grant No. LQ16F010007 and Project 61601152 supported by National Natural Science Foundation of China. The associate editor coordinating the review of this letter and approving it for publication was M. Caleffi.

The author is with the School of Communication Engineering, Hangzhou Dianzi University, Hangzhou 310018, China (e-mail: huaz@hdu.edu.cn).

Digital Object Identifier 10.1109/LCOMM.2017.2741462

In this letter, an antenna tilt adaptation approach for multi-cell massive MIMO systems is proposed. With pilot contamination, the spectral efficiency is firstly analyzed and its asymptotic expression in the limit of the BS antennas is also derived. Then, detailed analysis shows that the asymptotic spectral efficiency is a concave function of the tilt with some specific requirements on system parameters, which are realizable. Additionally, it is proved that there exists one global maximum point. According to these properties, a gradient descent based approach is proposed to search for the tilt with maximum spectral efficiency. Simulation results show that the proposed approach performs as well as the approach with exhaustive search and is better than a low-complexity approach.

Notations: Lower-case (upper-case) boldface symbols denote vectors (matrices); $(\cdot)^T$, $(\cdot)^*$, and $(\cdot)^H$ denote the transpose , the conjugate, and the conjugate transpose, respectively; $[\cdot]_j$, $[\cdot]_{j:l,n}$, and $[\cdot]_{j,l}$ are the jth row, the jth to the l-th elements in the n-th column, and the (j,l)-th element of a matrix, respectively; $\mathrm{sgn}(\cdot)$ is the sign of a number; $\mathcal{CN}(\mu,\sigma^2)$ is a circularly-symmetric complex Gaussian random variable with mean μ and variance σ^2; $\mathbb{E}\{\cdot\}$ denotes the expectation; and i is the imaginary unit.

II. System Model

Consider L rhomb shaped cells, each consists of one BS and K mobile stations (MSs). The BSs simultaneously serve the MSs. There are M antennas in the BS and each MS has one antenna. The antennas in the BS are directional and the antennas in the MSs are omnidirectional. The antennas in the BS are in the form of a uniform rectangular array, in front of which are the MSs. The numbers of antenna elements in the horizontal direction and the vertical direction of the array are N_{H} and N_{V}, respectively. Additionally, the array is vertical to the ground. The DOAs of the MSs are shown in Fig. 1, where $\theta^{\mathrm{az}}_{jlkp}$ is the azimuth DOA of the p-th path, $\theta^{\mathrm{el}}_{jlk}$ is the elevation DOA and is the same for all the paths. It is assumed that the scatters are distributed around the MS and are of the similar height as the MS, and the BS is much higher than the scatters, as urban cells without high buildings. Then, the angle spreads in the elevation plane are very small, as shown in [14]. Thus, the elevation DOAs of each MS are simplified as path-common. As can be seen, the larger the elevation DOA, the closer the MS gets to the BS. For MSs inside the j-th cell, the elevation DOA $\theta^{\mathrm{el}}_{jjk} \in [\theta^{\mathrm{in}}_{\min}, \theta^{\mathrm{in}}_{\max}]$. For MSs outside the j-th cell, the elevation DOA $\theta^{\mathrm{el}}_{jlk} \in [\theta^{\mathrm{out}}_{\min}, \theta^{\mathrm{in}}_{\min}]$.

The system operates in the time division duplex mode for channel reciprocity in the two-way links. Meanwhile, the channel is invariant in one coherent interval, in which the pilot and the data are transmitted. In the following, the antenna tilt is optimized for the uplink, the downlink can be optimized

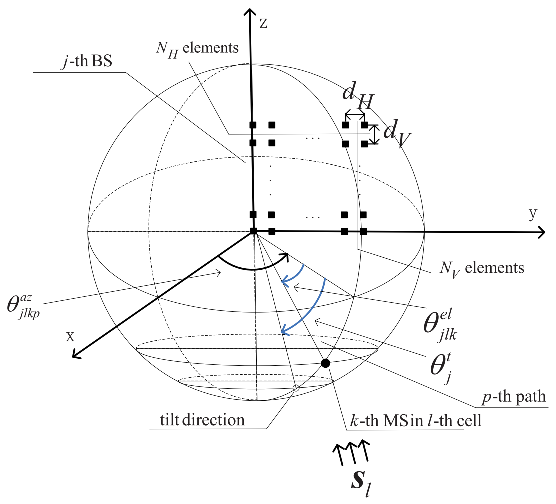

Fig. 1. The illustration of the array, the axes, and the DOAs.

similarly and is not analyzed here. Since the elevation DOAs and the large scale fading coefficients vary slowly, they are assumed to be known to the BS.

A. Transmission Process

In the channel estimation phase, the received pilots at the BS are given by $\mathbf{Y}_j = \sqrt{\rho}\sum_{l=1}^{L}\mathbf{H}_{jl}\tilde{\mathbf{D}}_{jl}\Phi^T + \mathbf{N}_j \in \mathbb{C}^{M\times K}$, where ρ is the power coefficient, $\mathbf{H}_{jl} \in \mathbb{C}^{M\times K}$ is the channel matrix, $\Phi \in \mathbb{C}^{K\times K}$ is the pilot matrix and satisfies $\Phi^T\Phi^* = \mathbf{I}_K$, $\mathbf{N}_j \in \mathbb{C}^{M\times K}$ is the noise matrix, which is composed of independent and identically distributed (i.i.d.) $\mathcal{CN}(0,\sigma_n^2)$ variables. Moreover, $\tilde{\mathbf{D}}_{jl} = \mathbf{D}_{jl}\mathbf{P}_l \in \mathbb{C}^{K\times K}$ is a matrix of the slowly varying variables, in which $\mathbf{D}_{jl} \in \mathbb{C}^{K\times K}$ is composed of the large scale fading coefficients from the MSs in the l-th cell to the j-th BS, and $\mathbf{P}_l \in \mathbb{C}^{K\times K}$ is composed of the power control variables of the MSs in the l-th cell. Note that $\mathbf{D}_{jl}$ and $\mathbf{P}_l$ are all diagonal matrices and the power control is set as $\mathbf{P}_l = \mathbf{D}_{ll}^{-1}$. The received signal is first processed with radio frequency (RF) beamforming using phase shifters and is converted to $\tilde{\mathbf{Y}}_j = \sqrt{\rho}\sum_{l=1}^{L}\tilde{\mathbf{H}}_{jl}\tilde{\mathbf{D}}_{jl}\Phi^T + \tilde{\mathbf{N}}_j \in \mathbb{C}^{N_{\mathrm{H}}\times K}$, where $[\tilde{\mathbf{Y}}_j]_{n,k} = \mathbf{w}_j^T[\mathbf{Y}_j]_{(n-1)N_{\mathrm{V}}+1:nN_{\mathrm{V}},k}$, $\mathbf{w}_j \in \mathbb{C}^{N_{\mathrm{V}}\times 1}$ is the RF beamforming vector, $\tilde{\mathbf{H}}_{jl} \in \mathbb{C}^{N_{\mathrm{H}}\times K}$, $[\tilde{\mathbf{H}}_{jl}]_{n,k} = \mathbf{w}_j^T[\mathbf{H}_{jl}]_{(n-1)N_{\mathrm{V}}+1:nN_{\mathrm{V}},k}$, $\tilde{\mathbf{N}}_j \in \mathbb{C}^{N_{\mathrm{H}}\times K}$, $[\tilde{\mathbf{N}}_j]_{n,k} = \mathbf{w}_j^T[\mathbf{N}_j]_{(n-1)N_{\mathrm{V}}+1:nN_{\mathrm{V}},k}$, where $n = 1,2,\cdots,N_{\mathrm{H}}$. The estimate of $\tilde{\mathbf{H}}_{jj}$ is obtained with pilot correlation as $\hat{\tilde{\mathbf{H}}}_{jj} \triangleq \rho^{-1/2}\tilde{\mathbf{Y}}_j\Phi^*\tilde{\mathbf{D}}_{jj}^{-1} \in \mathbb{C}^{N_{\mathrm{H}}\times K}$, and is written as $\hat{\tilde{\mathbf{H}}}_{jj} = \sum_{l=1}^{L}\tilde{\mathbf{H}}_{jl}\tilde{\mathbf{D}}_{jl}\tilde{\mathbf{D}}_{jj}^{-1} + \rho^{-1/2}\tilde{\mathbf{N}}_j\Phi^*\tilde{\mathbf{D}}_{jj}^{-1}$.

Similar to the pilot transmission, the received data vector at the BS is given by $\mathbf{y}_j = \sqrt{\rho}\sum_{l=1}^{L}\mathbf{H}_{jl}\tilde{\mathbf{D}}_{jl}\mathbf{s}_l + \mathbf{n}_j \in \mathbb{C}^{M\times 1}$, where $\mathbf{s}_l \in \mathbb{C}^{K\times 1}$ is composed of the data symbols transmitted by the MSs in the l-th cell, which are of variance one; $\mathbf{n}_j \in \mathbb{C}^{M\times 1}$ is the noise vector of i.i.d. $\mathcal{CN}(0,\sigma_n^2)$ variables. With RF beamforming, $\mathbf{y}_j$ is converted into $\tilde{\mathbf{y}}_j = \sqrt{\rho}\sum_{l=1}^{L}\tilde{\mathbf{H}}_{jl}\tilde{\mathbf{D}}_{jl}\mathbf{s}_l + \tilde{\mathbf{n}}_j \in \mathbb{C}^{N_{\mathrm{H}}\times 1}$, where $\tilde{\mathbf{n}}_j \in \mathbb{C}^{N_{\mathrm{H}}\times 1}$, $[\tilde{\mathbf{n}}_j]_{n,1} = \mathbf{w}_j^T[\mathbf{n}_j]_{(n-1)N_{\mathrm{V}}+1:nN_{\mathrm{V}},1}$. With the minimum mean square error (MMSE) principle, the detection matrix $\mathbf{T}_j \in \mathbb{C}^{K\times N_{\mathrm{H}}}$ is written as $\mathbf{T}_j = ((\hat{\tilde{\mathbf{H}}}_{jj}\tilde{\mathbf{D}}_{jj})^H\hat{\tilde{\mathbf{H}}}_{jj}\tilde{\mathbf{D}}_{jj} + \rho^{-1}\sigma_n^2\mathbf{I}_K)^{-1}(\hat{\tilde{\mathbf{H}}}_{jj}\tilde{\mathbf{D}}_{jj})^H$. Correspondingly, the processed data vector is $\check{\mathbf{y}}_j = \mathbf{T}_j\tilde{\mathbf{y}}_j = \sqrt{\rho}\sum_{l=1}^{L}\mathbf{T}_j\tilde{\mathbf{H}}_{jl}\tilde{\mathbf{D}}_{jl}\mathbf{s}_l + \mathbf{T}_j\tilde{\mathbf{n}}_j \in \mathbb{C}^{K\times 1}$. Note that the above process utilizes the three dimensional (3D) channel information and is usually called 3D beamforming, as in [13].

B. Channel Model

According to the previous presentation, it can be found that the channel is constituted with the channel matrix and the large scale fading coefficients. In particular, each column of the channel matrix is written as $[\mathbf{H}_{jl}]_{1:M,k} = \sum_{p=1}^{P} g_{jlkp}\sqrt{a_{jlkp}}\mathbf{b}(\theta^{\mathrm{az}}_{jlkp},\theta^{\mathrm{el}}_{jlk})$, where $g_{jlkp}, l = 1,2,\cdots,L, k = 1,2,\cdots,K, p = 1,2,\cdots,P$ are small scale fading variables and are i.i.d. $\mathcal{CN}(0,1)$ distributed; P is the number of paths; a_{jlkp} is the antenna gain, $\mathbf{b}(\theta^{\mathrm{az}}_{jlkp},\theta^{\mathrm{el}}_{jlk}) \in \mathbb{C}^{M\times 1}$ is the array steering vector. In particular, $10\log_{10}a_{jlkp} \triangleq A_{jlkp}$ is given as $A_{jlkp} = G_{\max} - \min\{-[A_{\mathrm{H}}(\theta^{\mathrm{az}}_{jlkp}) + A_{\mathrm{V}}(\theta^{\mathrm{el}}_{jlk})], A_{\mathrm{m}}\}$, where $G_{\max}$ is the maximum antenna gain, A_{m} is the side lobe level, $A_{\mathrm{H}}(\theta^{\mathrm{az}}_{jlkp}) = -\min\{12(\theta^{\mathrm{az}}_{jlkp}/\theta^{\mathrm{az}}_{3\mathrm{dB}})^2, A_{\mathrm{m}}\}$ is the horizontal antenna pattern, $\theta^{\mathrm{az}}_{3\mathrm{dB}}$ is the half power beamwidth in this pattern, $A_{\mathrm{V}}(\theta^{\mathrm{el}}_{jlk}) = -\min\{12(\theta^{\mathrm{el}}_{jlk}/\theta^{\mathrm{el}}_{3\mathrm{dB}})^2, SLA_{\mathrm{V}}\}$ is the uplink vertical antenna pattern, $\theta^{\mathrm{el}}_{3\mathrm{dB}}$ is the half power beamwidth in this pattern, SLA_{V} is the side lobe level in this pattern [14], [15]. Note that the elevation DOA here is 90° smaller than that in [14] and [15]. Additionally, $[\mathbf{b}(\theta^{\mathrm{az}}_{jlkp},\theta^{\mathrm{el}}_{jlk})]_{(n-1)N_{\mathrm{V}}+m,1} = \exp(i2\pi((n-1)d_{\mathrm{H}}/\lambda\cos(\theta^{\mathrm{el}}_{jlk})\sin(\theta^{\mathrm{az}}_{jlkp}) - (m-1)d_{\mathrm{V}}/\lambda\sin(\theta^{\mathrm{el}}_{jlk})))$, where d_{H} and d_{V} are the horizontal and the vertical antenna spacing, λ is the wavelength, $m = 1,2,\cdots,N_{\mathrm{V}}$. Meanwhile, the RF beamforming vector is defined as $[\mathbf{w}_j]_{m,1} = (1/\sqrt{N_{\mathrm{V}}})\exp(i2\pi(m-1)d_{\mathrm{V}}/\lambda\sin(\theta^{\mathrm{t}}_j))$, where θ^{t}_j is the uplink electrical antenna tilt of the j-th BS, which is the same as that in [15] and is 90° smaller than that in [14]. Note that when the tilt gets larger, the main lobe of the antenna pattern turns towards the bottom of the BS. Additionally, the tilt is adjustable in the range $\theta^{\mathrm{t}}_j \in [0°, 90°]$.

III. Tilt Adaptation

The existing tilt adaptation approaches are based on perfect CSI or require exhaustive search. Here, a convex optimization approach is proposed for tilt adaptation.

A. Spectral Efficiency

According to the expression of $\check{\mathbf{y}}_j$, the signal-to-interference-plus-noise ratio (SINR) of the k-th MS in the j-th cell in the uplink is $\gamma_{jk} = \rho\mathbb{E}\{|[\mathbf{T}_j\tilde{\mathbf{H}}_{jj}\tilde{\mathbf{D}}_{jj}]_{k,k}[\mathbf{s}_j]_{k,1}|^2\}/\mathbb{E}\{|\sqrt{\rho}f_{jk} + [\mathbf{T}_j]_k\tilde{\mathbf{n}}_j|^2\}$, where $f_{jk} = \sum_{l\neq j}[\mathbf{T}_j]_k\tilde{\mathbf{H}}_{jl}\tilde{\mathbf{D}}_{jl}\mathbf{s}_l + \sum_{k'\neq k}[\mathbf{T}_j\tilde{\mathbf{H}}_{jj}\tilde{\mathbf{D}}_{jj}]_{k,k'}[\mathbf{s}_j]_{k',1}$. According to the expressions in section II, it can be seen that $[\tilde{\mathbf{H}}_{jl}]_{n,k} = r_{jlk}\sum_{p=1}^{P} g_{jlkp}\sqrt{a_{jlkp}}[\mathbf{c}_{jlkp}]_{n,1}$, where

$$r_{jlk} = \frac{1-\exp(i2\pi d_{\mathrm{V}}/\lambda N_{\mathrm{V}}(\sin(\theta^{\mathrm{t}}_j) - \sin(\theta^{\mathrm{el}}_{jlk})))}{1-\exp(i2\pi d_{\mathrm{V}}/\lambda(\sin(\theta^{\mathrm{t}}_j) - \sin(\theta^{\mathrm{el}}_{jlk})))}, \quad (1)$$

$\mathbf{c}_{jlkp} \in \mathbb{C}^{N_{\mathrm{H}}\times 1}$, $[\mathbf{c}_{jlkp}]_{n,1} = (1/\sqrt{N_{\mathrm{V}}})\exp(i2\pi((n-1)d_{\mathrm{H}}/\lambda\cos(\theta^{\mathrm{el}}_{jlk})\sin(\theta^{\mathrm{az}}_{jlkp})))$. Then, we have

$$\frac{N_{\mathrm{V}}}{N_{\mathrm{H}}}\mathbf{c}^{H}_{jl'k'p'}\mathbf{c}_{jlkp} = \frac{1}{N_{\mathrm{H}}}\frac{1-\exp(i2\pi d_{\mathrm{H}}/\lambda\Delta)}{1-\exp(i2\pi d_{\mathrm{H}}/\lambda\Delta N_{\mathrm{H}})} \rightarrow \delta(l-l')\delta(k-k')\delta(p-p'),\ \text{as } N_{\mathrm{H}}\rightarrow\infty,$$

where $\Delta = \cos(\theta^{\mathrm{el}}_{jlk})\sin(\theta^{\mathrm{az}}_{jlkp}) - \cos(\theta^{\mathrm{el}}_{jl'k'})\sin(\theta^{\mathrm{az}}_{jl'k'p'})$. Thus, $N_{\mathrm{V}}/N_{\mathrm{H}}\tilde{\mathbf{H}}^{H}_{jl'}\tilde{\mathbf{H}}_{jl} \rightarrow \delta(l-l')\mathbf{X}_{jl} \in \mathbb{C}^{K\times K}$, where $\mathbf{X}_{jl}$ is a diagonal matrix and $[\mathbf{X}_{jl}]_{k,k} = |r_{jlk}|^2|\sum_{p=1}^{P} g_{jlkp}\sqrt{a_{jlkp}}|^2$. Then, the limiting SINR is $\bar{\gamma}_{jk} \triangleq \lim_{N_{\mathrm{H}}\rightarrow\infty}\gamma_{jk} = \upsilon_{jjk}|r_{jjk}|^4/(\sum_{l\neq j}\upsilon_{jlk}|r_{jlk}|^4)$, where $\upsilon_{jlk} = [\tilde{\mathbf{D}}_{jl}]^4_{k,k}|\sum_{p=1}^{P} g_{jlkp}\sqrt{a_{jlkp}}|^4$. As can be seen, the MMSE detection can eliminate the intra-cell interference but not the inter-cell interference. By adjusting the tilt, the ratio $|r_{jjk}|/|r_{jlk}|$ is adjusted, cf. (1), and the inter-cell interference can be mitigated. Hence, the asymptotic spectral efficiency in the uplink is $\bar{R} = \sum_{j=1}^{L}\sum_{k=1}^{K}\log_2(1+\bar{\gamma}_{jk})$.

B. Tilt Adaptation Approach

The objective of the tilt adaptation is to maximize the spectral efficiency. Thus, the tilt adaptation problem in the uplink is

$$\max_{\theta^{\mathrm{t}}_j, j=1,2,\cdots,L} \bar{R} \quad \text{s.t. } \theta^{\mathrm{t}}_j \in [\theta^{\mathrm{in}}_{\min}, \theta^{\mathrm{in}}_{\max}],\ j=1,2,\cdots,L. \tag{2}$$

Here, the uplink spectral efficiency is approximated as $\bar{R} \approx R = \sum_{j=1}^{L}\sum_{k=1}^{K}\log_2\left(1+1/\eta_{jk}\right)$. Correspondingly, $\bar{\gamma}_{jk}$ is approximated as

$$1/\bar{\gamma}_{jk} \approx \eta_{jk} = \sum_{l\neq j}\alpha_{jlk}\beta_{jlk}, \tag{3}$$

where $\beta_{jlk} = [\tilde{\mathbf{D}}_{jl}]^4_{k,k}\sum_{p=1}^{P}|a_{jlkp}|^2/([\tilde{\mathbf{D}}_{jj}]^4_{k,k}\sum_{p=1}^{P}|a_{jjkp}|^2)$, and

$$\alpha_{jlk} = 10^{0.4(B^{\mathrm{el}}_{jlk}-B^{\mathrm{el}}_{jjk})},$$

where $B^{\mathrm{el}}_{jlk} = -\min\{12((\sin(\theta^{\mathrm{t}}_j)-\sin(\theta^{\mathrm{el}}_{jlk}))/\tilde{\theta}_{3\mathrm{dB}})^2, \tilde{A}_{\mathrm{m}}\}$, $\tilde{A}_{\mathrm{m}} = 10$, $\tilde{\theta}_{3\mathrm{dB}} = x_0/(\tilde{A}_{\mathrm{m}}/12)^{1/2}$; $|r_{jlk}| \approx 0.1$ for $|\sin(\theta^{\mathrm{t}}_j) - \sin(\theta^{\mathrm{el}}_{jlk})| = x_0 < \lambda/d_{\mathrm{V}}/N_{\mathrm{V}}$, cf. (1). Here, $|r_{jlk}| \approx 10^{0.1B^{\mathrm{el}}_{jlk}}$ for small N_{V} and $\upsilon_{jlk} \approx [\tilde{\mathbf{D}}_{jl}]^4_{k,k}\sum_{p=1}^{P}|a_{jlkp}|^2$ for large P are used in the approximation.

Note that β_{jlk} is known, and only α_{jlk} is related to the tilts. Thus, the optimization problem in (2) can be partitioned into L problems, each of which is related to one of the tilts. For the tilt θ^{t}_j, the problem is

$$\max_{\theta^{\mathrm{t}}_j} R_j \quad \text{s.t. } \theta^{\mathrm{t}}_j \in [\theta^{\mathrm{in}}_{\min}, \theta^{\mathrm{in}}_{\max}], \tag{4}$$

where $R_j = \sum_{k=1}^{K}\log_2\left(1+1/\eta_{jk}\right)$ is the approximate uplink spectral efficiency of the j-th cell. Before presenting the proposed tilt adaptation approach, one proposition should be given first.

Proposition 1: According to the relation between $u_j = \sin(\theta^{\mathrm{t}}_j)$ and $b_{jlk} = \sin(\theta^{\mathrm{el}}_{jlk})$, for each combination of j,k, there are four cases, in which the case $|u_j - b_{jjk}| > x_0$, $|u_j - b_{jlk}| \leq x_0, \forall l \neq j$ is denoted as C1. With $x_{jlk} = \epsilon\alpha_{jlk}\beta_{jlk}$, $\epsilon = 9.6\ln 10/\tilde{\theta}^2_{3\mathrm{dB}}$, ϵ_0 is the maximum of $\epsilon_{0,jk}$ for j,k corresponding to C1, $\epsilon_{0,jk} = (\sum_{l\neq j}x_{jlk})^2/\sum_{l_2\neq j,l_2>l_1}\sum_{l_1\neq j}x_{jl_1k}x_{jl_2k}(b_{jl_1k}-b_{jl_2k})^2$, then ϵ_0 is related to R_j in the way that they are all functions of x_{jlk} and ϵ_0 influences the concavity of R_j. The physical meaning of ϵ_0 is that it is the inverse of a kind of weighted sum of the square of $b_{jl_1k} - b_{jl_2k}$, which is the difference between the sine values of the elevation DOAs for C1. When the SINR $1/\eta_{jk}$ tends to infinity, R_j below (4) tends to be a concave function of θ^{t}_j for $\epsilon > \epsilon_0$. In addition, there exists one $\theta_{\mathrm{mid}} \in [\theta^{\mathrm{in}}_{\min}, \theta^{\mathrm{in}}_{\max}]$ such that $\partial R_j/\partial u_j = 0$ when $\theta^{\mathrm{t}}_j = \theta_{\mathrm{mid}}$.

Proof: From the equation below (4), it can be found that $|\partial^2 R_j/\partial u^2_j - \sum_{k=1}^{K}p_{jk}/\ln 2| \leq \eta|\partial^2 R_j/\partial u^2_j|$ for $0<\eta<1$, where $\eta = \max\eta_{jk}$, $p_{jk} = \left(\partial\eta_{jk}/\partial u_j\right)^2/\eta^2_{jk} - \partial^2\eta_{jk}/\partial u^2_j/\eta_{jk}$. As $\eta_{jk} \rightarrow 0$, i.e., $\eta \rightarrow 0$, we have $\partial^2 R_j/\partial u^2_j \rightarrow \sum_{k=1}^{K}p_{jk}/\ln 2$. From the equations below (3), it can be found that $B^{\mathrm{el}}_{jlk} = -12((u_j - b_{jlk})/\tilde{\theta}_{3\mathrm{dB}})^2$, in case of $|u_j - b_{jlk}| \leq x_0$. Otherwise, $B^{\mathrm{el}}_{jlk} = -\tilde{A}_{\mathrm{m}}$. Accordingly, we have $\partial\eta_{jk}/\partial u_j = \sum_{l\neq j}x_{jlk}y_{jlk}$, $\partial^2\eta_{jk}/\partial u^2_j = \sum_{l\neq j}x_{jlk}z_{jlk}$. In addition, $y_{jlk} = b_{jlk} - u_j$, $z_{jlk} = \epsilon y^2_{jlk} - 1$ for the case C1. Note that the expressions of y_{jlk} and z_{jlk} in other cases are omitted here. Then, for cases other than C1, $p_{jk} \leq 0$. For C1, it can be found that $\eta^2_{jk}p_{jk} = (\sum_{l\neq j}x_{jlk})^2/\epsilon - \sum_{l_2\neq j,l_2>l_1}\sum_{l_1\neq j}x_{jl_1k}x_{jl_2k}(b_{jl_1k}-b_{jl_2k})^2$. Thus, for $\epsilon > \epsilon_0$, there is $\epsilon > \epsilon_{0,jk}$, then we have $p_{jk} < 0$. Then, $\partial^2 R_j/\partial u^2_j < 0$, which means R_j tends to be a concave function of θ^{t}_j. Similarly, as $\eta_{jk} \rightarrow 0$, we have $\partial R_j/\partial u_j \rightarrow \sum_{k=1}^{K}q_{jk}$, where $q_{jk} = -\epsilon/\ln 2\sum_{l\neq j}x_{jlk}y_{jlk}/\sum_{l\neq j}x_{jlk}$. The derivative demonstrates that the maximum of R_j reaches at $\theta^{\mathrm{t}}_j \geq \theta^{\mathrm{in}}_{\min}$. Since R_j is asymptotically concave, there exists one $\theta_{\mathrm{mid}} \in [\theta^{\mathrm{in}}_{\min}, \theta^{\mathrm{in}}_{\max}]$ such that $\partial R_j/\partial u_j = 0$ when $\theta^{\mathrm{t}}_j = \theta_{\mathrm{mid}}$. ■

Remark 1: As $\max(b_{jl_1k} - b_{jl_2k})^2 \approx \tilde{\theta}^2_{3\mathrm{dB}}\tilde{A}_{\mathrm{m}}/3$, we have $\min\epsilon_{0,jk} \approx 3(L-1)^2/(\tilde{A}_{\mathrm{m}}\tilde{\theta}^2_{3\mathrm{dB}})$ with approximately equal x_{jlk}. With $L = 3$, $\tilde{\theta}_{3\mathrm{dB}} = 0.28$, and $\tilde{A}_{\mathrm{m}} = 10$, we have $\min\epsilon_{0,jk} \approx 15.3$, $\epsilon \approx 282$. Then, $\epsilon > \min\epsilon_{0,jk}$. Typically, $\alpha_{jlk} = 1.1\times 10^{-3}$, $\beta_{jlk} = 6.7\times 10^{-5}$. Then, $\eta_{jk} = 1.474\times 10^{-7}$, cf. (3).

If the k-th MSs in the j-th and the l-th cells are near the cell edge and are close, $\eta_{jk} \approx 1$; Otherwise, $1/\eta_{jk} \gg 1$ usually holds, cf. (3) and the equations below. As the probability of the first condition is low, the SINR is usually large, and as shown with the typical values in the remark above. Thus, the concavity of the uplink spectral efficiency with respect to tilt is realizable. Moreover, the physical intuition of C1 is that the tilt, θ^{t}_j, is away from the elevation DOA of the MS inside the cell, $\theta^{\mathrm{el}}_{jjk}$, and is close to that of the MS outside the cell, $\theta^{\mathrm{el}}_{jlk}$. Typically, the search range of the tilt is $\theta^{\mathrm{t}}_j \in [4.86°, 40.36°]$, the ranges of the elevation DOAs are $\theta^{\mathrm{el}}_{jjk} \in [4.86°, 40.36°]$ and $\theta^{\mathrm{el}}_{jlk} \in [2.11°, 4.86°]$. As can be seen, the probability of θ^{t}_j being close to $\theta^{\mathrm{el}}_{jlk}$ is low, i.e., the probability of C1 is expected to be very low. Thus, the restriction on ϵ may be relaxed. Then, a gradient descent based method that uses the backtracking line search algorithm in [16] is applied, which is Algorithm 1.

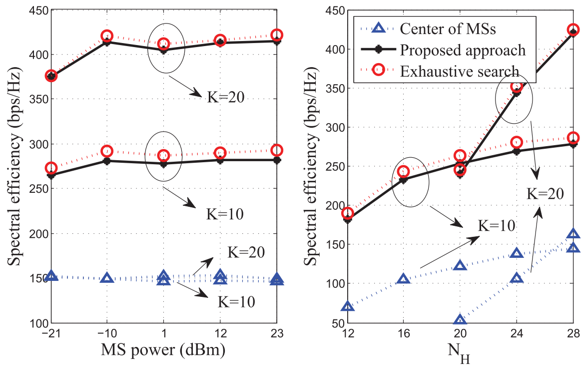

Fig. 2. The illustration of the spectral efficiencies versus the average MS Tx power and the number of horizontal antennas.

Algorithm 1 Uplink Tilt Adaptation Algorithm

Initialize: $u_j^{(1)} = \sin(\max(\theta_{jjk}^{\mathrm{el}}, \forall k))$, $\Delta = x_0$,$\xi = 0.1$, $n = 1, \eta = 0.5, \zeta_{j,n} = 1$, calculate R_j with $u_j = u_j^{(1)}$

1: **while** $\Delta > \xi$ and $\zeta_{j,n} \neq 0$

2: $n \leftarrow n+1, \Delta \leftarrow 2\Delta, \delta_R = -1$

3: **while** $\delta_R \leq -10^{-5}$

4: $\Delta \leftarrow 0.5\Delta$,$\zeta_{j,n} = \partial R_j / \partial u_j|_{u_j = u_j^{(n-1)}}$

5: $u_j = u_j^{(n-1)} + \mathrm{sgn}(\zeta_{j,n})\Delta$, calculate B_{jlk}^{el}

6: Calculate $\tilde{R}_j$ by changing R_j with $\tilde{R}_j$ in (6)

7: Calculate $\delta_R = \tilde{R}_j - R_j - \eta\Delta|\zeta_{j,n}|$

8: **end while**

9: $R_j \leftarrow \tilde{R}_j$, $u_j^{(n)} \leftarrow u_j^{(n-1)} + \mathrm{sgn}(\zeta_{j,n})\Delta$

10: **end while**

11: $\theta_j^{\mathrm{t}} \leftarrow \arcsin(u_j^{(n)})$

IV. Simulation Results

In the simulations, $L = 3$ and the cell topology is similar to that in [9]. The system parameters are set as the 3D urban micro cell scenario in [14]. The radius of the cell (from BS to edge) is 100 meters, the minimal distance from the MS to the BS is 10 meters. The height of the BS is 10 meters. All the MSs are outdoor, and the MS height is 1.5 meters. The path loss is set according to the non line of sight model. The thermal noise spectral density is -174 dBm/Hz. The bandwidth is 10 MHz. The average transmission power of each MS, i.e., the average MS Tx power, is 23 dBm. Other parameters are $N_{\mathrm{H}} = 28$, $N_{\mathrm{V}} = 7$, $\theta_{3\mathrm{dB}}^{\mathrm{az}} = 65°$, $\theta_{3\mathrm{dB}}^{\mathrm{el}} = 65°$, $A_{\mathrm{m}} = 30$, and $SLA_{\mathrm{V}} = 30$, $G_{\max} = 8$ dBi, $P = 20$, $d_{\mathrm{H}} = d_{\mathrm{V}} = \lambda/2$. The "center of MSs" approach is similar to that in [11], with the tilt as the mean of the elevation DOAs of all the MSs in the cell. The "exhaustive search" approach is similar to that in [9] and [10], which searches exhaustively in the effective tilt range.

The spectral efficiencies versus the MS Tx power and the number of horizontal antennas are shown in Fig. 2. The spectral efficiency of the proposed approach is similar to that of the "exhaustive search" approach and is higher than that of the "center of MSs" approach. This verifies that the near optimal tilts can be achieved with the proposed approach and also means that the proper adaptation of the tilts can mitigate the interference.

V. Conclusion

In this letter, the spectral efficiency of the system is analyzed and is proved to be concave of the tilt. Then, a gradient descent based approach is proposed to achieve the approximately optimal tilt.

Acknowledgment

The author gratefully acknowledge the many helpful comments of the three anonymous reviewers and Editor Dr. George Alexandropoulos.

References

[1] F. Rusek *et al.*, "Scaling up MIMO: Opportunities and challenges with very large arrays," *IEEE Signal Process. Mag.*, vol. 30, no. 1, pp. 40–60, Jan. 2013.

[2] T. L. Marzetta, "Noncooperative cellular wireless with unlimited numbers of base station antennas," *IEEE Trans. Wireless Commun.*, vol. 9, no. 11, pp. 3590–3600, Nov. 2010.

[3] L. Lu, G. Y. Li, A. L. Swindlehurst, A. Ashikhmin, and R. Zhang, "An overview of massive MIMO: Benefits and challenges," *IEEE J. Sel. Topics Signal Process.*, vol. 8, no. 5, pp. 742–758, Oct. 2014.

[4] S. Saur and H. Halbauer, "Exploring the vertical dimension of dynamic beam steering," in *Proc. 8th Int. Workshop Multi-Carrier Syst. Solutions (MC-SS)*, Herrsching, Germany, May 2011, pp. 1–5.

[5] H. Halbauer, S. Saur, J. Koppenborg, and C. Hoek, "Interference avoidance with dynamic vertical beamsteering in real deployments," in *Proc. IEEE Wireless Commun. Netw. Conf. Workshops (WCNCW)*, Paris, France, Apr. 2012, pp. 294–299.

[6] J. Koppenborg, H. Halbauer, S. Saur, and C. Hoek, "3D beamforming trials with an active antenna array," in *Proc. Int. ITG Workshop Smart Antennas*, Dresden, Germany, Mar. 2012, pp. 110–114.

[7] H. Halbauer, S. Saur, J. Koppenborg, and C. Hoek, "3D beamforming: Performance improvement for cellular networks," *Bell Labs Tech. J.*, vol. 18, no. 2, pp. 37–56, Sep. 2013.

[8] A. Imran, M. A. Imran, A. Abu-Dayya, and R. Tafazolli, "Self organization of tilts in relay enhanced networks: A distributed solution," *IEEE Trans. Wireless Commun.*, vol. 13, no. 2, pp. 764–779, Feb. 2014.

[9] N. Seifi, M. Coldrey, and M. Viberg, "Throughput optimization for MISO interference channels via coordinated user-specific tilting," *IEEE Commun. Lett.*, vol. 16, no. 8, pp. 1248–1251, Aug. 2012.

[10] N. Seifi, J. Zhang, R. W. Heath, Jr., T. Svensson, and M. Coldrey, "Coordinated 3D beamforming for interference management in cellular networks," *IEEE Trans. Wireless Commun.*, vol. 13, no. 10, pp. 5396–5410, Oct. 2014.

[11] A. Müller, J. Hoydis, R. Couillet, and M. Debbah, "Optimal 3D cell planning: A random matrix approach," in *Proc. IEEE Global Commun. Conf. (GLOBECOM)*, Anaheim, CA, USA, Dec. 2012, pp. 4512–4517.

[12] W. Lee, S.-R. Lee, H.-B. Kong, S. Lee, and I. Lee, "Downlink vertical beamforming designs for active antenna systems," *IEEE Trans. Commun.*, vol. 62, no. 6, pp. 1897–1907, Jun. 2014.

[13] A. Kammoun, H. Khanfir, Z. Altman, M. Debbah, and M. Kamoun, "Preliminary results on 3D channel modeling: From theory to standardization," *IEEE J. Sel. Areas Commun.*, vol. 32, no. 6, pp. 1219–1229, Jun. 2014.

[14] 3GPP, "Study on 3D channel model for LTE," 3GPP TSG, Valbonne, France, Tech. Rep. 3GPP TR 36.873 V12.0, Sep. 2014.

[15] 3GPP, "Study of radio frequency (RF) and electromagnetic compatibility (EMC) requirements for active antenna array system (AAS) base station," 3GPP TSG, Valbonne, France, Tech. Rep. 3GPP TR 37.840 V12.1, Dec. 2013.

[16] S. Boyd and L. Vandenberghe, *Convex Optimization*. Cambridge, U.K.: Cambridge Univ. Press, 2004.